Journal of Applied Spectroscopy, Vol. 73, No. 5, 2006

DOUBLE PULSE UV LASER INDUCED BREAKDOWN SPECTROSCOPY OF STAINLESS STEEL

A. A. I. Khalil,[1,2*] M. Richardson,[2] C. Barnett,[3] and L. Johnson[3]

UDC 535.33:669.14

Results of experimental investigations of 304 austenitic stainless steel (ASS) ultraviolet spectral range by single and double pulse laser induced breakdown spectroscopy (LIBS) at atmospheric pressure are reported. Various parameters, such as laser energy, placement of the laser beam focus with respect to the surface of illumi- nation, and collinear double laser pulse delay were used as variables. This study contributes to a better under- standing of the LIBS plasma dynamics by observing the temporal evolution of various emission lines. Temperature measurements were made by the Boltzmann diagram method using singly ionized Fe lines, and electron densities were found from Stark broadening. The temporal behaviors of these parameters were also estimated. It was found that the electron temperature for double pulses is higher than that for single pulse of the same total energy. For double pulse LIBS, the iron line emission intensities are enhanced and the analytical performance is improved. For instance, the intensity of iron line Fe I 275.01 nm was a factor of about 300 times higher if a double pulse of 2 × 20 mJ was used instead of a single pulse of 40 mJ when focusing the beam 4.7 mm behind the target surface.

Key words: *Nd:YAG laser, double pulse, LIBS, stainless steel target.*

Introduction. Laser induced breakdown spectroscopy (LIBS) is becoming one of the most promising new tools for rapid spectrochemical analysis in the steel industry. It offers solutions to a large number of analytical problems. It is an inexpensive quantitative method for the remote analysis of liquid [1] and high temperature steel [2, 3], and for depth profiling of coated steel. Due to their excellent high-temperature strength [4], heat-resistant stainless steels are widely used in many emerging technologies and, on a large scale, in manufacturing electrical appliances, nuclear, hospital, furniture, and surgical equipment, at petrochemical plants, and in the automotive industry. Therefore, it is important to improve instrumental analysis techniques for real-time monitoring of steel production. With LIBS, analysis of the emitted lines allows the direct analysis of the material's atomic composition.

In this paper, we document the temporal evolution and dynamics of UV LIBS plasma by studying several parameters of iron neutral and ion lines in austenitic stainless steel (ASS) spectrum as a function of focus distance with respect to the surface of the target, the time interval between laser pulse and ICCD camera gate width, and the laser energy ratio of the two pulses. In contrast to many previous studies, the spectral range was selected in the UV region. The primary plasma parameters, viz., electron temperature (T_e) and density (n_e), have been estimated for both single- and double-pulse (SP and DP) modes. DP LIBS can yield greatly enhanced emission signals, along with improving signal-to-noise ratios, produces much lower detection limits, enhances plasma emission lifetimes, and reduces systematic errors in quantitative analysis.

Experimental Setup. 304 ASS targets were irradiated by the focused 532-nm output of two up-converted Q-switched Nd:YAG lasers [5] yielding beams 5 mm in diameter. The schematic diagram of the experimental setup for the DP LIBS experiment is shown in Fig. 1. The pulse of the laser 1 (initial beam) is of 6 nsec duration and maxi-

*To whom correspondence should be addressed.

[1]Department of Laser Industrial Applications, National Institute of Laser Enhanced Science (NILES), Cairo University, Giza, Egypt. E-mail: mcr@creol.ucf.edu; [2]Laser Plasma Laboratory, College of Optics & Photonics, University of Central Florida, Orlando, USA; [3]Department of Physics, Florida A&M University, Tallahassee, USA. Published in Zhurnal Prikladnoi Spektroskopii, Vol. 79, No. 5, pp. 654–660, 2006. Original article submitted March 14, 2006.

0021-9037/06/7305-0735 ©2006 Springer Science+Business Media, Inc.

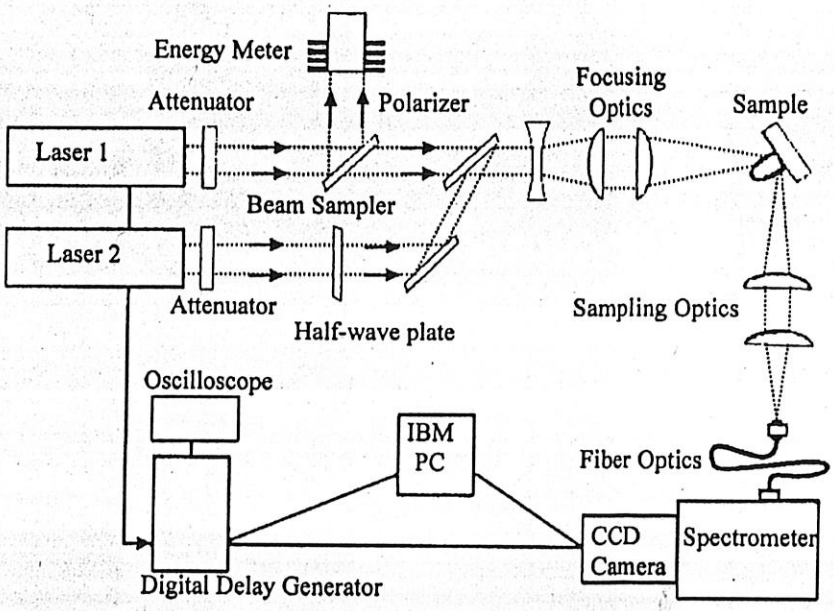

Fig. 1 Schematic diagram of the experimental setup.

mum energy of 150 mJ, and that of the second laser 2 (delayed beam) — 8 nsec and 300 mJ, respectively. Both lasers were operated at a 10 Hz repetition rate and were tested for the maximum of achievable spatial resolution. A Stanford Research System, model DG535, delay generator synchronized Q-switches of both lasers. The firing time jitter between the two lasers was <10 nsec.

Both lasers were equipped with variable beam attenuators to control the pulse energy. They illuminated the target collinearly. Typically, pulse energies of ~40 mJ and 20 mJ respectively for each laser have been used. Placing a large pixel sensor array into the focal plane of the spectrograph permitted the simultaneous detection of many lines of interest with a high spectral resolution and, in turn, multi-element analysis. To produce a more de- fined focus, both beams were expanded by a ratio of 3:1 with a simple Galilean telescope before the final focus lens, an A/R-coated fused silica plano-convex singlet lens (f = 200 mm). Each beam was incident to the ASS foil at 36°. The focal spot diameter of each beam was 100–200 μm. The waist of the beam focus was positioned onto the surface of the target. The target in the form of a slightly polished slab was translated to provide a fresh surface for every 10 shots, over which a spectrum was obtained. Emission from the plasma was image relayed by two plano-convex lenses (f = 75 mm) to a fiber bundle, which illuminated the entrance slit of a 30-cm, f/4 spectrometer [6]. The fiber bundle is 1 m long and consists of 19–200 μm diameter fibers arranged in a single column at one end. A holographic grating of 2400 grooves/mm blazed at 500 nm for the UV and visible has been installed in order to analyze the steel plasma plume. These experimental LIBS-investigations of Q-switched SP- and DP-induced plasma of 304 ASS in UV region from 262 to 285 nm at atmospheric pressure are reported for the first time. The spectra were recorded by a gated intensified CCD detector. The ICCD camera (Andor Technologies) was thermoelectrically cooled to –15°C and had an effective size of 690 × 128 pixels and a minimum gate width of 30 nsec. Gate delays were changed to observe the plasma temporal evolution, while gate widths were kept at 50 nsec. Single emission lines were observed with a photomultiplier tube [7] with the signal being recorded using a 1-GHz oscilloscope (Model 744). The pulsed laser radiation with peak intensity of about 10^{11} W/cm^2 creates dense plasma. The ASS targets square in shape measured 5 × 5 × 0.1 cm^3. The single laser spot on the ASS surface was about 4 μm deep. The measurements were performed after cleaning the surface from contamination several times. The steel had the following chemical composition: 0.08 wt % C, 1 wt % Si, 2 wt % Mn, 0.045 wt % P, 0.03 wt % S, 18 wt % Cr, 8 wt % Ni, and 70.84 wt % Fe.

Time dependences of emission intensities of atomic (Fe I, $5D$–$5P^*$, 275.01 nm) and ionic (Fe II, $2D$–$2F^*$, 267.03 nm) emission lines have been studied. The background was constant in all cases and amounted to 1650 a.u. In our measurements, this value was subtracted from the emission spectra intensities. All the spectroscopic data corre-

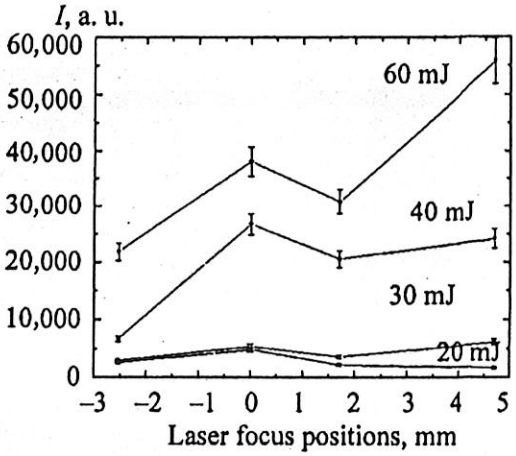

Fig. 2 Relative intensity of Fe I 275.01 mm spectral line at different SP laser focus positions (2.54 mm in front of the sample, on surface, 1.7 mm behind the surface, 4.7 mm behind the surface).

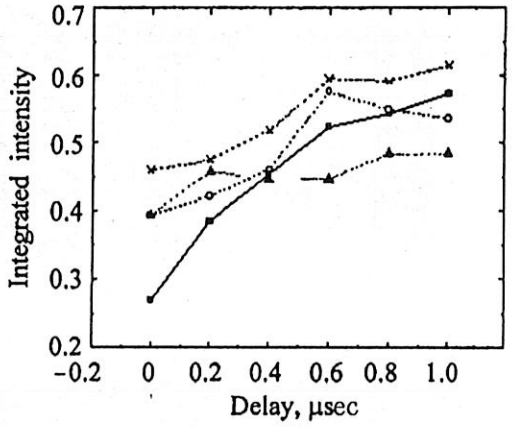

Fig. 3 Integrated intensity of Fe I 275.01 nm line for different focus positions from the surface as a function of delay between B_1 (20 mJ) and B_2 (40 mJ): 2.54 mm in front of the surface (■), on the surface (○), 1.7 mm behind the surface (▲), 4.7 mm behind the surface (×).

sponding to the investigated emission lines of stainless steel species have been obtained from the NIST spectroscopic database.

Results and Discussion. The dynamic, transient behavior of the LIBS-plasma is challenging for diagnostics since its fundamental parameters vary dramatically in time and position. We performed spectral analysis and traced temporal evolution of ASS UV emission using LIBS technique. The primary purpose of this study was to obtain the optimum experimental conditions for LIBS by subjecting stainless steel to the laser beam. We searched for the best way to extend the plasma lifetime and to enhance the emission intensity of the plasma by varying the laser focus positions with respect to the target surface in air.

Figure 2 shows the relative intensity of the Fe I (275.01 nm) spectral line as a function of the laser focus position. It can be seen that the relative intensity has maximum at 0 position for laser energies of 20, 30, 40 mJ except that the curve for 60 mJ has two maxima at 0 and 4.7 mm. The error bar is about 7 %. The relative intensity at 60 mJ is higher than that at 20 mJ by a factor of 10 at 4.7 mm. This implies that the ideal position to obtain

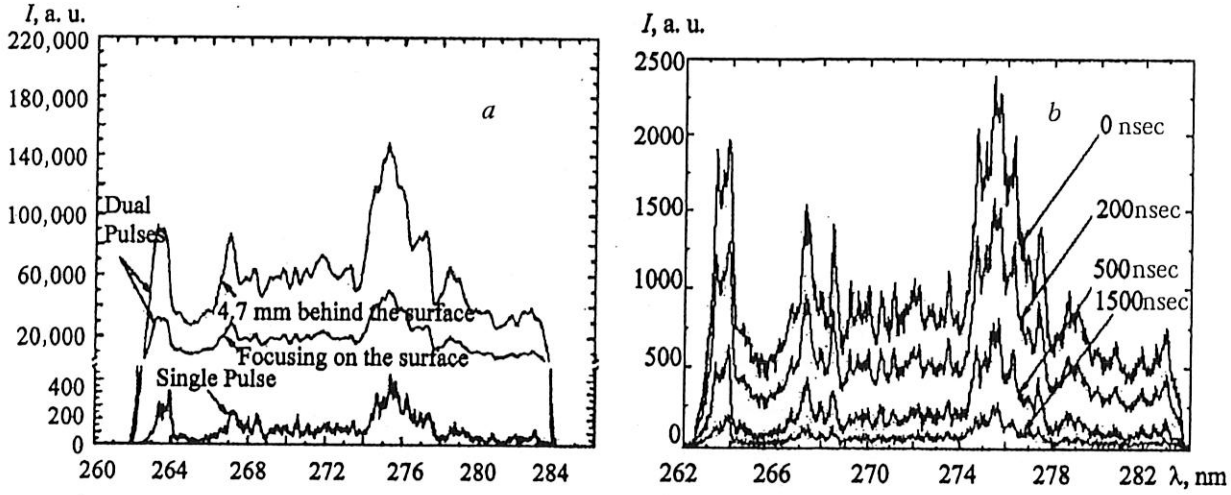

Fig. 4 Spectra taken for both SP and DP 0.5 μsec after initial pulse by focusing laser beams on the target surface and 4.7 mm behind the surface (a) and plasma emission spectra in the wavelength range 262 to 284 nm taken with different time delays (b). The time delays correspond to the time after the laser pulse maximum.

higher spectral intensity is 4.7 mm behind the surface. The measured signal intensity increases slowly with the laser energy in the low energy range and rapidly at higher energies as shown in Fig. 2. The difference in the intensity values at lower energies in the range 20–30 mJ is less than that at higher energies in the range 30–60 mJ. It was observed that the length of the plasma plume increases with the laser energy. Figure 3 illustrates the integrated intensity of the DP emission of the Fe I 275.01 nm spectral line for both lasers of 20 mJ and 40 mJ at different focus positions from the surface.

Figure 4a shows the spectral intensity of the Fe I 275.01 nm line for SP and DP (delay time between the second pulse and CCD camera gate width is 0.5 μsec) focused on the surface and 4.7 mm behind the surface. The intensity of iron line Fe I 275.01 nm is a factor of about 60 and 300 times higher for a DP than for a SP of the same total energy focused on the target surface and 4.7 mm behind the surface. Time resolved spectra were recorded by setting the gate width to 50 nsec and laser focusing on the target surface at a laser irradiance of $1.35 \cdot 10^{10}$ W·cm^{-2}. Typical spectra, as recorded at different regimes of the plasma expansion, are shown in Fig. 4b.

Figure 5 shows the temporal evolution of the Fe lines from 0 to 6000 nsec. It can be seen that after the laser pulse <200 nsec, the plasma emission consists in an intense signal that decreases with time for SP as shown in Fig. 5a. For the SP, no maximum was observed. However, in Fig. 5b, in the case of DP, the emission intensity follows the same pattern for both Fe I and Fe II (275.01 and 267.03 nm) and reaches the same maximum for the 500-nsec delay with the focus 2.54 mm in front of the sample, on the sample, and 4.7 mm behind the sample, respectively, plus another maximum at delay time of 1000 nsec 1.7 mm behind the surface. When the lasers are focused on the surface as shown in Fig. 5b, twin peaks are obtained in the temporal profile of Fe I in laser-produced ASS plasma in air. The emission lines of Fe I and Fe II decrease gradually at the higher delay time. At longer times >3000 nsec, the ion lines disappear.

The excitation temperature can be determined with the well-known Boltzmann method from relative line intensities, provided that their transition probabilities (A_{jk}) from a given excitation state are known. The electron temperature was measured from the emission intensities of five iron (Fe I) lines shown in Table 1. These lines are well resolved, with well-known uncertainties of their respective transition probabilities.

A prerequisite to the electron temperature measurement is as follows: the plasma meets the conditions for local thermodynamic equilibrium (LTE) and is optically thin for the lines observed. Therefore, the populations of the excited states follow a Boltzmann distribution, and their relative emissivity (ε_{jk}) can be given by [10, 11]:

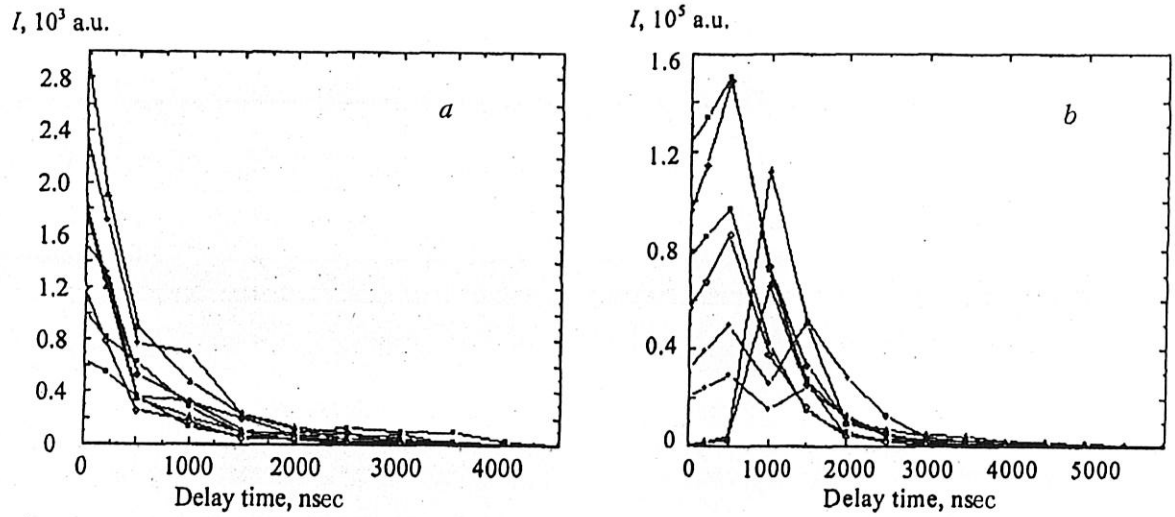

Fig. 5 Time dependence of the emission intensities of Fe atomic (275.01 nm) and Fe^+ ionic (267.03 nm) emission lines for SP (a) and DP (b) in air at atmospheric pressure: Fe(I) 2.54 mm in front of the surface (■), Fe(II) 2.54 mm in front of the surface (□), Fe(I) on the surface (•), Fe(II) on the surface (○), Fe(I) 1.7 mm behind the surface (▲),Fe(II) 1.7 mm behind the surface (△), Fe(I) 4.7 mm behind the surface (♦), Fe(II) 4.7 mm behind the surface (◇).

TABLE 1. Spectroscopic data of prominent analyst and reference Fe I lines used for calculating the ASS plasma temperature of [12]

λ_{jk}, nm	E_k, eV	E_j, eV	g_j	A_{jk}, 10^8 sec^{-1}
263.2594	0.080	4.783	5	0.015
273.548	0.912	5.431	7	0.620
274.406	0.121	4.626	3	0.350
275.010	0.050	4.546	7	0.390
278.810	0.857	5.290	13	0.630

$$\ln\left(\frac{\lambda_{jk}\varepsilon_{jk}}{A_{jk}g_j}\right) = -\frac{E_j}{kT_{\text{exc}}} + \ln\left(\frac{N(T)}{Q(T)}\right) \tag{1}$$

where A_{jk}, λ_{jk} and g_j are the transition probability, wavelength, and the statistical weight for the upper level, respectively; E_j is the excited level energy; T_{exc} is the excitation temperature; k and h are the Boltzmann and Planck constants, respectively; $Q(T)$ is the partition function and $N(T)$ is the atomic (or ion) density. The wavelengths, degeneracies, transition probabilities, statistical weights, and excitation energies for these iron lines are summarized in NIST on the atomic spectra database [12]. The plasma temperature can be calculated from the slope of the line obtained by plotting the energy (E_j) versus the natural logarithm of the parameters as shown in Eq. (1).

A typical Boltzmann plot used to calculate the temperature is given in Fig. 6a. Figure 6b illustrates the temporal evolution of the measured excitation temperature. This temperature exhibits an initial fast decay for SP from 2900 K at 0 μsec to 2100 K at 0.5 μsec and slightly decreases over the range from 1 to 5 μsec where the Fe lines finally disappear. Also, the temperature for the DP exhibits fast decay from 4700 K at 0.5 μsec to 3000 K at 1 μsec

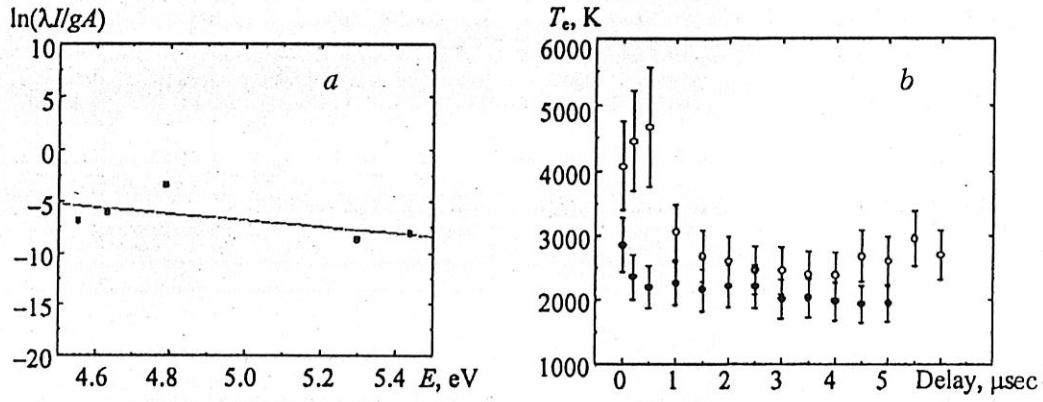

Fig. 6 (a) Typical Boltzmann plot used for estimating the plasma temperature: 500 nsec (■), 3361 K (—), 2.5 mm in front of the surface, (b) time-resolved excitation temperature of plasma for DP (open circles) and for SP (filled circles) at 4.7 mm behind the surface. The laser intensity was $1.35 \cdot 10^{10}$ W/cm^2.

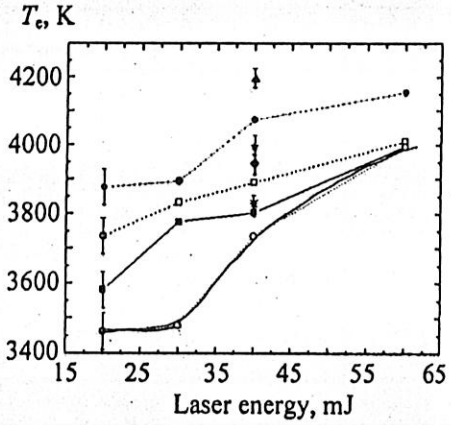

Fig. 7 Electron temperature for SP and DP as a function of the laser energy for different laser focus positions: 2.54 mm in front of the surface SP (■), on the surface SP (□), 1.7 mm behind the surface SP (○), 4.7 mm behind the surface SP (•), 2.54 mm in front of the surface DP (*), on the surface DP (♦), 1.7 mm behind the surface DP (×), 4.7 mm behind the surface DP (▲).

and then slightly decreases to 2700 K at 6 μs. The statistical error bar for the excitation temperature may be less than 5% over several experimental measurements.

Figure 7 shows the electron temperature for SP and DP (interpulse separation of DP is 0.5 μsec) as a function of the total laser energy. The electron temperature determined for SP action increases with laser energy at all positions. The difference in electron temperatures at different positions is higher at the lower laser energies and decreases at higher energies as shown in Fig. 7.

Density Measurement Using Stark Broadening. The spectroscopic technique to determine electron density (N_e) depends upon the measurement of the stark broadening of some optical lines [13]. The Stark width parameter (ω) of the selected spectral line was determined experimentally [14]. The full width at half maximum (FWHM) $\Delta\lambda_{1/2}$ of the Stark broadened line of neutral atom is given by [15, 16]

$$\Delta\lambda_{1/2}\,(A) = 2\omega\,(N_e/10^{16}) \qquad (2)$$

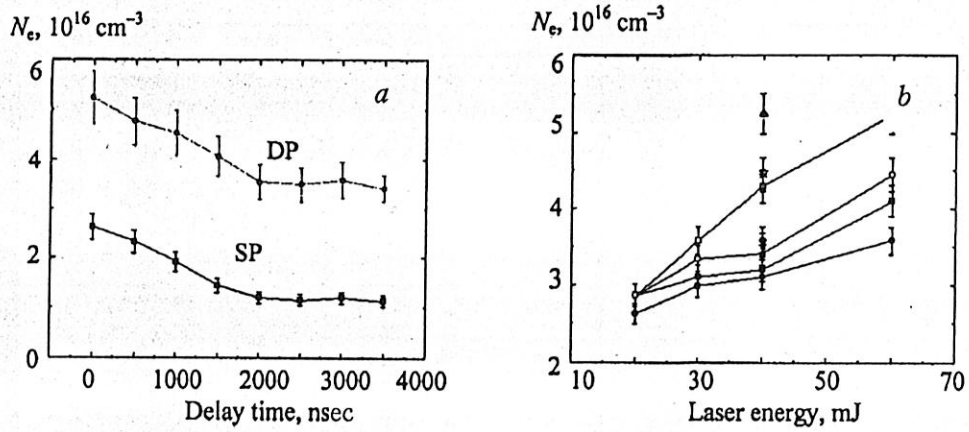

.Fig. 8 Electron density for SP and DP deduced from the Fe I 275.01 nm line as a function of the plasma delay time (a) and the total energy at different focus positions with DP delay time of 0.5 μs (b): 2.54 mm in front of the surface SP (■), on the surface SP (○), 1.7 mm behind the surface SP (•), 4.7 mm behind the surface SP (□), 2.54 mm in front of the surface DP (*), on the surface DP (♦), 1.7 mm behind the surface DP (×), 4.7 mm behind the surface DP (▲).

where A and N_e are the ion broadening parameter and the electron number density in cm^{-3}. Both ω and A are weak functions of temperature.

The line width was determined by a Lorentzian profile numerical fitting. Figure 8a shows the measured electron densities for SP and DP as a function of delay time when laser focusing at 4.7 mm behind the surface. From 0 to 3500 nsec, the electron density decreases from $2.6 \cdot 10^{16}$ to $1.13 \cdot 10^{16}$ cm^{-3} for SP while for DP — from $5.3 \cdot 10^{16}$ to $2.62 \cdot 10^{16}$ cm^{-3}. It can be seen that the electron density in the case of DP is higher than in the case of SP. The profile obtained reveals nearly linear decay in electron density between 0 and 3500 nsec.

For SP, the electron density increases with the rise in pulse energy to ~60 mJ for all the laser focus positions and amounts to $3.2 \cdot 10^{16}$, $3.4 \cdot 10^{16}$, $3.1 \cdot 10^{16}$, and $4.29 \cdot 10^{16}$ cm^{-3} at 2.54 mm in front of the surface, on the surface, at 1.7 mm and 4.7 mm behind the surface, respectively, as shown in Fig. 8b. For DP, the electron density is higher than in the case of SP and equals to $3.5 \cdot 10^{16}$, $3.6 \cdot 10^{16}$, $4.5 \cdot 10^{16}$, and $5.3 \cdot 10^{16}$ cm^{-3} for different positions at constant energy.

Conclusion. The double pulse LIBS technique was used to characterize the laser-produced plasma from ASS in air. The spectral intensity as a function of pulse delay time, laser pulse energy, and laser focus position from the target surface was temporally measured. In the in-line geometry studied, the optimal placement of the laser focal spot was found to be behind the target surface. It was observed that the intensity of iron line Fe I 275.01 nm was a factor of about 60 and 300 times higher if double pulses were used instead of single pulses and laser focus was on the target surface and at 4.7 mm behind the target surface, respectively. It was also noticed that the plasma lifetime for single and double pulses was different, the lifetime in the case of double pulses being longer by a factor of two than that in the case of single pulses. The double laser pulse clearly produced hotter and denser plasma at the same amount of laser energy. In order to optimize the method and analytical performance when studying such plasmas, one needs to use short delay times and sufficiently high laser fluencies and adjust the laser focus position relative to the target surface.

Acknowledgment. A.A.I. Khalil thanks the IDB of Saudi Arabia for a Post-Doctoral research fellowship.

REFERENCES

1. J. Gruber, J. Heitz, H. Strasser, D. Bauerle, N. Ramaseder. *Spectrochim. Acta B*, **56**, 685 (2001).
2. S. Palanco, L. M. Cabal'm, D. Romero, J. J. Laserna. *J. Anal. At. Spectrom.*, **14**, 1883 (1999).

3. H. Bette, R. Noll, G. Mueller, H. Jansen, C. Nazikkol, H. Mittelstaedt. *J. Laser Appl.*, **17**, No. 3, 183–190 (2005).
4. *In Stainless Steel*, Ed. R.A.Lula, American Society for Metals (1986)
5. http://www.bigskylaser.com/brilliantseries.html
6. http://www.roperscientific.de/datasheets/PurgedSP300.pdf
7. http://www.hamamatsu.com
8. G. Bekefi, C. Deutsch, B. Yaakobi, in: "*Principles of Laser Plasmas*," Ed.G. Bekefi, New York, Wiley Interscince, Ch. 13 (1994), p. 549.
9. J. A. Aguilera and C. Aragon. *Spectrochim. Acta, B*, **59**, 1861 (2004).
10. P. W. J. M. Boumans, in: "*Theory of Spectrochemical Excitation*," Ed. P. W. J. M. Boumans, London, Hilger and Watts, Ch. 6 (1966), p. 92.
11. W. Lochte-Holtgreven, in: "*Plasma Diagnostics*," Ed. W. Lochte-Holtgreven, New York, Wiley Interscience, Ch. 3 (1968), p. 135.
12. http://www.nist.gov
13. G. Bekefi, in: "*Principles of Laser Plasmas*," Ed. G. Bekefi, New York, Wiley Interscience, Ch. 13 (1976), p. 549.
14. N. Konjevic and W. L. Wiese. *J. Phys. Chem. Ref. Data*, **19**, 1307 (1990).
15. H. R. Griem. *Spectral Line Broadening by Plasmas*, New York, Academic (1974).
16. D. B. Chrisey and G. K. Hubler. *Pulsed Laser Deposition of Thin Films*, New York,Wiley, Ch. 5 (1994).
17. H. Balzer, M. Hoehne, V. Sturm, R. Noll. *Spectrochim. Acta B*, **60**, 1172–1178 (2005)